

Calibration of a Bio-optical Model in the North River, North Carolina (Albemarle–Pamlico Sound): A Tool to Evaluate Water Quality Impacts on Seagrasses

Patrick D. Biber · Charles L. Gallegos ·
W. Judson Kenworthy

Received: 3 January 2007 / Revised: 28 August 2007 / Accepted: 12 November 2007 / Published online: 18 December 2007
© Coastal and Estuarine Research Federation 2007

Abstract Seagrasses are typically light limited in many turbid estuarine systems. Light attenuation is due to water and three optically active constituents (OACs): nonalgal particulates, phytoplankton, and colored dissolved organic matter (CDOM). Using radiative transfer modeling, the inherent optical properties (IOPs) of these three OACs were linked to the light attenuation coefficient, K_{PAR} , which was measured in North River, North Carolina, by profiles of photosynthetically active radiation (PAR). Seagrasses in the southern portion of Albemarle-Pamlico Estuarine System (APES), the second largest estuary in the USA, were found to be light limited at depths ranging from 0.87 to 2 m. This corresponds to a range of K_{PAR} from 0.54 to 2.76 m^{-1} measured during a 24-month monitoring program. Turbidity ranged from 2.20 to 35.55 NTU, chlorophyll *a* from 1.56 to 15.35 $mg\ m^{-3}$, and CDOM absorption at 440 nm from 0.319 to 3.554 m^{-1} . The IOP and water quality data

were used to calibrate an existing bio-optical model, which predicted a maximum depth for seagrasses of 1.7 m using annual mean water quality values and a minimum light requirement of 22% surface PAR. The utility of this modeling approach for the management of seagrasses in the APES lies in the identification of which water quality component is most important in driving light attenuation and limiting seagrass depth distribution. The calibrated bio-optical model now enables researchers and managers alike to set water quality targets to achieve desired water column light requirement goals that can be used to set criteria for seagrass habitat protection in North Carolina.

Keywords Seagrass · Optical model · Water quality · Albemarle–Pamlico Sound · Turbidity · Chlorophyll · Colored dissolved organic matter

P. D. Biber (✉)
Institute of Marine Science,
University of North Carolina at Chapel Hill,
3431 Arendell St.,
Morehead City, NC 28557, USA
e-mail: patrick.biber@usm.edu

C. L. Gallegos
Smithsonian Environmental Research Center,
P.O. Box 28, Edgewater, MD 21037, USA
e-mail: gallegosc@si.edu

W. J. Kenworthy
Center for Coastal Fisheries and Habitat Research, NOS, NOAA,
101 Pivers Island Road,
Beaufort, NC 28516, USA
e-mail: jud.kenworthy@noaa.gov

Introduction

Estuaries and coastal waters are highly productive, ecologically, and socially valuable ecosystems. They are under increasing stress from anthropogenic factors, such as nutrient enrichment and sediment loading, which both affect water clarity and primary production. Seagrasses are important benthic primary producers that are strongly affected by water quality (Dennison et al. 1993; Abal and Dennison 1996) and play a central role in the stability, nursery function, biogeochemical cycling, and trophodynamics of coastal ecosystems. As such, they are important for sustaining a broad spectrum of organisms (Thayer et al. 1984; Hemminga and Duarte 2000; Larkum et al. 2006).

Seagrasses are widely recognized as indicators of estuarine health, being perhaps the most sensitive indicator of estuarine water quality throughout the range of their distribution (Dennison et al. 1993; Biber et al. 2005). For this reason, Dennison et al. (1993) concluded that seagrasses were potentially sensitive indicators of declining water quality primarily because of their higher light requirements than those of other aquatic primary producers, such as macroalgae and benthic microalgae (Duarte 1991; Markager and Sand-Jensen 1992, 1994, 1996; Agusti et al. 1994; Gattuso et al. 2006).

Provided that the habitat is suitable for seagrass growth (e.g., wave exposure, current speed, tidal range, sediment quality; see Koch 2001), the light environment during the growing season is probably the most important abiotic factor determining survival of seagrasses in degraded coastal waters (Moore et al. 1997; Batiuk et al. 2000; Dixon 2000). Light attenuation by the water column is a major variable related to seagrass distribution and abundance (Kenworthy and Haunert 1991; Kenworthy and Fonseca 1996; Steward et al. 2005). The area of seagrass coverage and particularly the maximum colonization depth are therefore important measures of seagrass condition driven by the optical water quality present within the system (Morris et al. 2000; Virnstein and Morris 2000; Biber et al. 2005).

Water clarity can be measured in a number of ways, e.g., Secchi depth or photosynthetically active radiation (PAR) attenuation coefficient; however, these measurements do not by themselves reveal anything about the components of water quality that cause light attenuation. Therefore, it is nearly impossible to use such measurements to set management goals for specific substances to achieve the desired water quality necessary to protect seagrasses.

To help predict seagrass depth distributions, we have developed and calibrated an optical water quality model based on the absorption and scattering of light by specific components in optically complex coastal waters (Gallegos 1994, 2001; Gallegos and Kenworthy 1996; Gallegos and Biber 2004). The model is formulated in terms of inherent optical properties (IOPs), which depend only on the contents of the water (i.e., the absorption, scattering, and backscattering coefficients). In contrast, apparent optical properties (AOPs) are dependent on the ambient light field (the diffuse attenuation coefficient, etc.). Radiative transfer modeling (Mobley 1994) provides the linkage between AOPs and IOPs, as well as environmental conditions. Our optical model is based on the IOPs of three optically active constituents (OACs; in addition to water itself): nonalgal particulates (NAP), phytoplankton, and colored dissolved organic matter (CDOM). The effect of each OAC is scaled by a water quality measurement that is easily made by management-oriented monitoring programs. For instance,

turbidity satisfies the criterion of a water quality measurement that is easily accessible to managers and is simultaneously a useful predictor of certain IOPs needed for site-specific calibration of a bio-optical model.

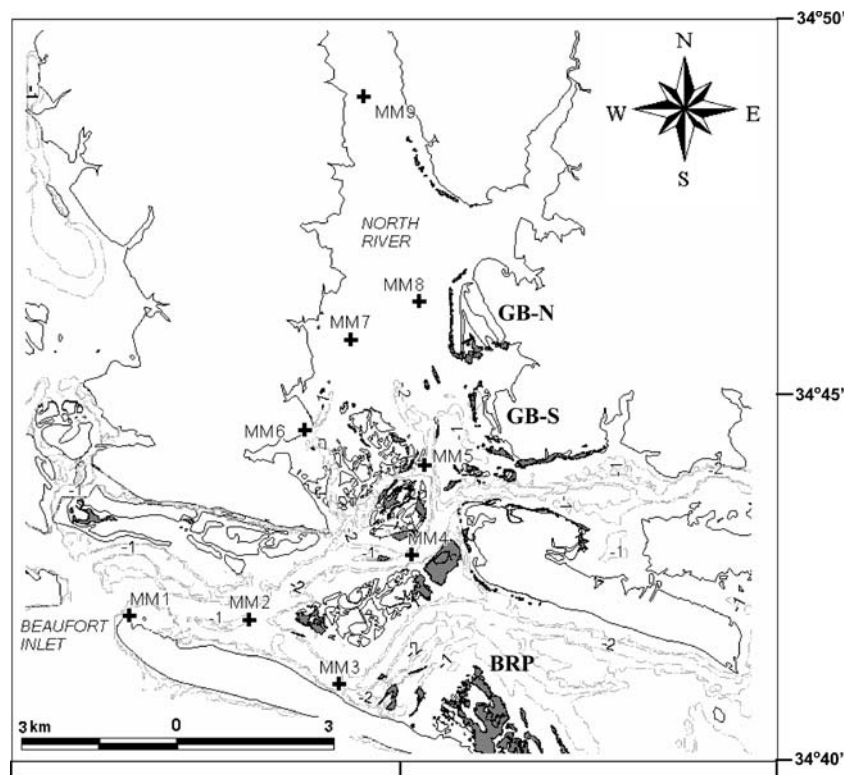
From prior studies, we know that low light levels, below some minimum physiological requirement (typically 15 to 40% of incident surface light), may result in depth-limited distribution and abundance of seagrasses (Dennison et al. 1993; Kenworthy and Fonseca 1996; Onuf 1996; Steward et al. 2005). With this information, the calibrated optical model may be inverted to set threshold concentrations for water quality parameters that meet the photosynthetic requirements for seagrasses at a given water depth. This is termed the water column light requirement or WCLR (Gallegos and Moore 2000).

We have used this optical model (Gallegos 1994, 2001; Gallegos and Kenworthy 1996) to generate WCLR targets based on the relative contributions of the three OACs within two estuaries, Chesapeake Bay and Indian River Lagoon (IRL). One of the main findings of this comparative research was that IOPs of particulate matter differ between the two systems, primarily because of changes in inorganic particle size and composition (Gallegos 1994; Gallegos and Moore 2000; Gallegos and Neale 2002). In this paper, we further determine regional differences in IOPs by working in a sub-basin of the nation's second largest estuarine system, the Albemarle–Pamlico Sound Estuary System (APES), North Carolina, which also supports the second greatest area of seagrass habitat nationally, after Florida (Green and Short 2003; Street et al. 2005). Our aim was to obtain a regionally customized diagnostic tool for North Carolina seagrasses, based on direct measurement of particulate and dissolved absorption spectra and optical modeling. A calibrated bio-optical model is needed to quantify the contribution of each water quality parameter to light attenuation (K_{PAR}). It is only from this calibration that WCLR thresholds of water quality parameters can be derived that are protective of seagrasses over a range of desired depths. Using these thresholds, managers can now determine whether the current state of the APES is protective of seagrass, and if not, they can determine the reduction in specific water quality parameters, i.e., turbidity and chlorophyll, needed to achieve a desired management goal without the need for additional complex optical measurements.

Study Site

The North River (North Carolina, USA) is a small submerged river estuary in the southern portion of the APES system, near Beaufort, NC (34°45'N, 76°35'W, Fig. 1). The North River is hydrologically connected to the southern Pamlico Sound through Back and Core

Fig. 1 Nine water quality sampling stations (MM1–MM9) and three seagrass deep-edge locations (GB-N, GB-S, BRP) in North River, North Carolina. One- and two-meter depth contours and the approximate distribution of most seagrass beds are shown in *dark gray shading*



Sounds, both areas rich in seagrass coverage (Ferguson and Wood 1994). Furthermore, the North River conveniently captures the range of water clarity and optical properties that characterize the much larger and experimentally less tractable APES system (Buzzelli et al. 2003; Lin et al. 2007). Along the distribution of seagrasses in North River, water quality changes from clearer coastal water at well-flushed stations near the Beaufort Inlet (station MM1) to highly colored and often turbid conditions in the interior of the estuary at station MM9, located adjacent to the Highway 70 bridge and causeway (Fig. 1). The North River bathymetry ranges from shallow mud bottom (mean depth 1 m) in the northern portion to deeper tidal channels with coarse textured sand substrates (mean depth 5 m) in the southern lower reaches nearest to Beaufort Inlet. Tidal currents are influenced by the Beaufort Inlet and extend up to about stations MM5 and 6 (Hench and Luettich 2003) resulting in marked and visible mixing of clearer coastal waters with turbid, highly colored estuarine waters (Biber, personal observation). The mean tidal range is 70 cm, but wind and barometric pressure gradients can cause larger changes in water level.

The North River system was also chosen because of known multidecadally stable seagrass beds occurring primarily in shallow waters fringing the salt marsh islands known as the Middle Marsh (Kenworthy et al. 1982; Carraway and Priddy 1983). The Middle Marshes are a flood tide delta formed by the Beaufort Inlet when it was

located further east than its current position on Shackleford Banks (Susman and Heron 1979). This island is part of the southern portion of the Outer Banks barrier islands (Pilkey and Fraser 2003), which form the outer protective barrier of the APES system against the Atlantic Ocean and have allowed seagrass meadows to flourish here during the Holocene.

Materials and Methods

For optical and water quality analyses, duplicate 4-L water samples were collected from a depth of 0.5 m at nine stations in North River (Fig. 1) at approximately monthly intervals from September 2002 to late August 2004. Additionally, at each station, we profiled water quality at 0.5-m increments from the surface to the bottom with a YSI® 6600 multiparameter probe (temperature, salinity, dissolved oxygen, pH, turbidity, and chlorophyll fluorescence) and simultaneously collected light attenuation data using a LICOR® 4π sensor tied to the YSI and attached to a LI-COR 1000 logger. The light data were used to calculate the diffuse attenuation coefficient for PAR, K_{PAR} , using the Lambert–Beer law:

$$PAR_z = PAR_0 \exp[-K_{PAR}z] \quad (1)$$

where PAR_0 and PAR_z are the PAR fluxes just below the water surface and at depth z , respectively. We calculated

K_{PAR} as the slope of a regression of $\ln(\text{PAR}_z)$ against z . Measured attenuation coefficients were used for evaluation of model predictions of K_{PAR} from relationships developed between IOP (absorption and scattering coefficients) and water quality measurements, as done previously (Gallegos 1994, 2001) and summarized below.

Bio-optical Model Development

Light absorption by different components is additive, proportional to the concentration of the causal agent, and a function of wavelength, λ . Therefore, we can write the total absorption as the sum of absorption spectra,

$$a_t(\lambda) = a_w(\lambda) + a_g(\lambda) + a_\phi(\lambda) + a_{p-\phi}(\lambda) \quad (2)$$

where a is the absorption coefficient and the subscripts t , w , g , ϕ , and $p-\phi$, stand for, respectively, total, water, CDOM, phytoplankton, and NAPs. The representation of the spectral variability is simplified by defining the normalized absorption spectrum for the water quality constituents, which are defined as the absorption at wavelength λ divided by the absorption at a reference wavelength, λ_c . Additionally, it is convenient to reference total absorption to absorption by water, as that is how available instrumentation measures it. That is,

$$a_{t-w}(\lambda) = a_g(440)g(\lambda) + a_\phi(675)\phi(\lambda) + a_{p-\phi}(440)p(\lambda) \quad (3)$$

where a_{t-w} is the total absorption less that due to pure water, and the functions $g(\lambda)$, $\phi(\lambda)$, and $p(\lambda)$ describe the spectral shape of absorption spectra due to CDOM, phytoplankton, and NAP respectively. The spectral shape functions have a value of 1 (dimensionless) at the reference wavelengths of 440 nm for CDOM, 675 nm for phytoplankton, and 440 nm for NAP.

The final step in relating the absorption spectrum to standard water quality measurements is to determine the scaling between the absorption coefficient at the reference wavelength and a correlated water quality measurement, chlorophyll a (Chl a) for phytoplankton, and turbidity (Turb) for NAPs (absorption by CDOM is expressed directly in absorption units). We can then write

$$a_{t-w}(\lambda) = a_g(440)g(\lambda) + a_\phi^*(675) \times [\text{chl } a] \times \phi(\lambda) + a_{\text{NTU}}^*(440) \times \text{Turb} \times p(\lambda) \quad (4)$$

where coefficients with asterisks are scale factors that relate absorption at the reference wavelength to water quality measurements. The scale factor for NAP absorption deserves special mention. Unlike $a_\phi^*(675)$, which has units $\text{m}^2 (\text{mg Chl } a)^{-1}$, $a_{\text{NTU}}^*(440)$ is not a true specific-absorption coefficient because turbidity is not a mass

concentration measurement. We used turbidity as a scaling water quality measurement because, as is often the case (Gallegos 1994; Gallegos and Kenworthy 1996), it was a better predictor of NAP absorption than total suspended solids (TSS) concentration. While it is true that phytoplankton can contribute to the output of a turbidity sensor, they are less efficient at backscattering than mineral particulates (Stramski et al. 2002). Furthermore, some contribution of phytoplankton to turbidity is beneficial because the nonpigmented organic carbon from phytoplankton that remains on a filter pad after solvent extraction also contributes to what is measured as “nonalgal” particulate absorption.

Scattering by particulate matter is treated in a similar manner as absorption. That is, the spectral shape of particulate scattering is defined by an empirical normalized scattering function, $b_n(\lambda)$, referenced to a characteristic wavelength. Thus, we represent the scattering spectrum as

$$b_p(\lambda) = b_{\text{NTU}}^*(555) \times \text{Turb} \times b_n(\lambda) \quad (5)$$

where $b_p(\lambda)$ is the scattering coefficient at wavelength λ , and the scattering/turbidity ratio, $b_{\text{NTU}}^*(555)$, relates scattering at the reference wavelength, 555 nm, to the turbidity, Turb.

Quantifying the Optically Active Constituents

To characterize the IOPs described above in the laboratory, we measured absorption, $a_{t-w}(\lambda)$, and beam attenuation coefficients, $c_{t-w}(\lambda)$, on one of two duplicate 4-L water samples collected from each station using a WETLabs ac-9 absorption-attenuation meter with a 25-cm flow tube, at wavelengths 412, 440, 488, 510, 532, 555, 650, 676, and 715 nm. To avoid bubble entrainment, water was gravity fed through the instrument at a flow rate of about 1.5 L min^{-1} , and data were logged for up to 90 s using the manufacturer’s Wetview software. Absorption coefficients were corrected for temperature and salinity as described in the instrument manual and for scattering as described by Gallegos and Neale (2002). Particulate scattering, $b_p(\lambda)$, was calculated from the difference, $b_p(\lambda) = c_{t-w}(\lambda) - a_{t-w}(\lambda)$. Whenever $c_{t-w}(412)$ was greater than 30 m^{-1} , samples were diluted 1:2 serially until measurements fell below that limit to keep samples within the manufacturer’s stated dynamic range. Final coefficients were scaled by the appropriate dilution factor.

Using the second 4-L water sample, we determined absorption of separate OAC by filtration. We measured absorption by particulate matter, $a_p(\lambda)$, using the quantitative filter pad technique of Kishino et al. (1985). A volume of water was filtered onto a 25-mm glass fiber filter (Whatman GF/F) and shipped on dry ice overnight to the Smithsonian Environmental Research Center laboratory

where they were stored frozen (-20°C) for less than 4 weeks. For measurements, filters were thawed and rewetted with 200 μL of filtered distilled water and placed next to the exit window of the sample beam of a Cary spectrophotometer. Absorbance was measured relative to a moistened blank GF/F filter placed next to the exit window of the reference beam. Measured absorbances were converted into in situ particulate absorption coefficients by multiplying by 2.303 [i.e., $\ln(10)$] and dividing by the geometric path length (=volume filtered/area of filter) and division by a path length amplification factor, $\beta=1.5$ (Tzortziou et al. 2006), determined by comparing filter pad measurements with measurements made on a solution contained inside an integrating sphere (Babin and Stramski 2002).

We measured absorption by CDOM using water filtered through a 0.22- μm pore-diameter polycarbonate membrane filter (Poretics) using 10-cm pathlength quartz cells (30 ml) referenced to a similarly filtered distilled water blank in an Ocean Optics USB2000 spectrophotometer. Measurements in absorbance units (AU) were converted to in situ absorption coefficients, $a_g(\lambda)$, by multiplying by 2.303 and dividing by the path length, 0.1 m.

For determination of chlorophyll concentrations (Chl a), duplicate 50-ml whole-water samples were filtered onto GF/F filters and stored frozen up to 4 weeks. Filters were thawed and extracted in 90% acetone overnight at 4°C in the dark. Chlorophyll concentrations, uncorrected for phaeo-pigments, were calculated from fluorometric measurements using a calibrated TD700 fluorometer corrected for volume filtered (EPA Method 445.0, revision 1.2).

In situ measurements of turbidity, using the YSI 6136 nephelometric sensor, were used in the model calibration, instead of TSS measurements, because of its correlation with scattering properties of the water (Kirk 1980, 1988) and the widespread use of this method (EPA Method 180.1, revision 2) in water quality monitoring.

Bio-optical Model Calibration

The calibration exercise is then reduced to determination of mean spectral shape functions, $g(\lambda)$, $\phi(\lambda)$, $p(\lambda)$, and $b_n(\lambda)$, from measured absorption and scattering spectra and the scaling coefficients $a_{\phi}^*(675)$, $a_{\text{NTU}}^*(440)$, and $b_{\text{NTU}}^*(555)$ from the linear regression of, respectively, $a_{\phi}(675)$ against Chl a , $a_{p-\phi}(440)$ against turbidity, and $b_p(555)$ against turbidity. We used forced zero-intercept regressions because a zero value must necessarily produce a zero optical signal. We used these coefficients in Eqs. 4 and 5 to predict absorption and scattering spectra and a modified version of the spreadsheet model of Gallegos (2001) to predict K_{PAR} from absorption and scattering spectra. Modeled K_{PAR} was then compared to the observed K_{PAR} .

Using the calibrated bio-optical model, we computed a “partial attenuation coefficient” for the contribution of each water quality parameter at each station to the annual mean K_{PAR} by successively substituting each measured annual mean value into the bio-optical model while setting the other two inputs to zero. In doing so, we allowed for covariation between chlorophyll and the other input parameters. That is, the presence of chlorophyll entails some amount of CDOM and turbidity, which must be added for the chlorophyll-only calculation and, similarly, removed when zeroing out chlorophyll. We calculated the chlorophyll-covarying CDOM from equation 18 of Morel and Maritorena (2001) and chlorophyll-covarying turbidity from their relationship between scattering coefficient and chlorophyll (equation 9 of Morel and Maritorena 2001) divided by our estimated value of $b_{\text{NTU}}^*(555)$. We used annual means because together the growing seasons of *Zostera marina* (near the southern limit of its distribution) and *Halodule wrightii* (near the northern limit of its distribution) encompass nearly the entire year.

From the “partial attenuation coefficients,” we computed the relative contribution to K_{PAR} of water alone and each water quality parameter individually, as the “partial attenuation coefficient” less that because of water alone, divided by the K_{PAR} with all three components at their annual mean. Calculated in this way, the sum of the “partial attenuation coefficients” is greater than 1 because of the inherent nonlinearity in the attenuation process. The fractions, nevertheless, give an accurate indication of the relative importance of the three determinants of the diffuse attenuation coefficient.

We used the calibrated bio-optical model to determine WCLR thresholds for seagrass beds in the APES system by inversion of the spreadsheet model. To do this, it is necessary to assume a physiological light requirement as a

Table 1 Water depths (cm) measured ($n=9$) and recorded at the three deep-edge locations, Goose Bay North (GB-N), Goose Bay South (GB-S), and Bottle Run Point (BRP) using a measuring stick, pressure sensors, and differentially corrected GPS data

Location	Transect	Depth measured Mean \pm SE	Pressure sensor ^a	MSL Local (D-GPS)
GB-N	1	86.89 \pm 0.92	84.10	Data error ^b
	2	73.22 \pm 1.02		Data error ^b
	3	70.11 \pm 1.63		Data error ^b
GB-S	1	84.44 \pm 1.24	72.26	85.5
	2	74.11 \pm 1.45		75.1
	3	69.67 \pm 0.69		70.8
BRP	1	68.44 \pm 0.47	69.96	67.1
	2	66.56 \pm 0.75		72.8
	3	66.44 \pm 1.00		70.0

^a Mean water depth over the 1.5-h collection period

^b Not reported as D-GPS not in carrier-phase mode

percentage of incident sunlight and a maximum depth for seagrass growth. Then, for a range of Chl *a* concentrations, we used the Solver routine in Excel™ to determine the turbidity value that predicts the assumed percentage of surface-incident light to penetrate to the assumed depth. We used 22% (Carter et al. 2000) for the seagrass physiological light requirement, with a fixed CDOM absorption at 0.694 m^{-1} (its average value for station MM5). We computed WCLR thresholds for depths of 1, 1.7, and 2 m mean sea level (MSL); these depths were selected based on information about seagrass deep-edge depths in the APES (Table 2). More recent discussions of seagrass light requirements suggest that 22% may be a minimum requirement and that 30–40% is a more realistic requirement for growth (Steward et al. 2005). If this is holds true, our use of 22% in the model calculations will result in WCLR thresholds that are only minimally protective of seagrasses; water quality values would need to be even lower than the thresholds we give in this paper.

Model Verification with Deep-edge Depths

To assess the bio-optical model predictions of seagrass depth based on observed water quality and the assumed 22% light requirement, three well-defined seagrass meadows were selected for surveying deep edges based on prior field assessments and aerial imagery (NASA 2002). These were Goose Bay North (GB-N: $34^{\circ}44.5102\text{N}$, $76^{\circ}35.3838\text{W}$) and Goose Bay South (GB-S: $34^{\circ}43.9095\text{N}$, $76^{\circ}35.0844\text{W}$) and Bottle Run Point (BRP: $34^{\circ}40.2846\text{N}$, $76^{\circ}34.5958\text{W}$; Fig. 1). We installed Odyssey Dataflow pressure sensors (accuracy= ± 0.8 mm), one per station, and left them to record depth at 5-min intervals over a period of 12 days to measure tidally averaged water depths at the deep edge. The vented sensors were placed at the sediment surface and were fastened to 2.54-cm-diameter steel conduit pipes pushed about 0.5 m into the soft sediments and raising the vent tubing orifice a minimum of 1 m above mean high high

water to permit correction for atmospheric pressure changes. On the day of sensor installation at the three sites, we sampled three transects spaced about 25 m apart using the self-contained underwater breathing apparatus (SCUBA). Along each transect line, we chose three adjacent quarter-meter square quadrats perpendicular to the deep edge to determine Braun–Blanquet assessments of seagrass coverage. These data were then used to confirm that sensors had been placed on the edge of the seagrass meadow. The pressure readings from the sensors were independently validated by measuring the water depth at the sensor repeatedly over the time it took to do the Braun–Blanquet assessments.

To further validate the mean deep-edge water depths derived from the pressure sensors, seagrass meadow deep-edge bathymetry was measured using the differential-global positioning system (D-GPS) phase carrier technique of Johansson (2002) and referenced to local MSL. A suitable tidally referenced geodetic benchmark was located at Harkers Island Ranger Station (SAM3) providing precise elevation and tidal references for the base station. After the deep-edge position was located using SCUBA (see above), the rover GPS was set up, and static satellite observations were conducted for a period sufficiently long to ensure that the rover and base stations collected at least 45 min of overlapping data. The satellite data collected on the GPS rover and base station units was later analyzed using the Trimble Pathfinder Office software to automatically calculate the relative elevation difference between the benchmark and the seagrass deep edge from the MTL elevation of the benchmark corrected for the antenna height.

Results

Spatial and Temporal Patterns of Water Quality

Surface water quality measurements (0–1 m) from the YSI 6600 multiparameter probe were used to determine the seasonal water quality dynamics of the North River, North Carolina, system. Spring was defined as 1 March to 31 May, summer as 1 June to 31 August, fall as 1 September to 30 November, and winter as 1 December to 28 February. Temperature followed an approximate sinusoidal pattern during the year with minimum temperatures in January and February and maximum temperatures in July and August. Salinity was higher and more stable in the downstream, oceanic influenced section of North River than the upstream portion, which was influenced by terrestrial runoff from surrounding salt marsh-dominated tributary streams. Salinity dropped after heavy rainfall events, especially during the wet spring and summer of 2003; this year was the wettest on record with 2,337 mm of precipitation recorded, 50% greater than the average (NOAA 2003). We

Table 2 Range of the maximum depths (m) referenced to MSL for meadow deep-edges from three different studies on seagrass distribution in the southern APES region: North River, North Carolina, and two shorelines of Core Sound

Study	Location	Range (m)
This paper	North River	0.80–0.98
Ferguson and Korfmacher 1997	Core Sound—western	≤ 1.2
	Core Sound—eastern	≤ 2.0
Field, unpublished data	Core Sound—eastern	1.8–2.2 ^a

^aData were not tidally corrected to MSL; half tidal amplitude is approximately 0.4 m

observed a spatial trend of increasing turbidity and Chl *a*, from the downstream (MM1) to the upstream station (MM9), but seasonal patterns were evident as well, with lower values noted in winter (Dec–Feb) than other seasons.

K_{PAR} values increased from the Beaufort Inlet at station MM1 to the upstream station at MM9, where turbidity, Chl *a*, and CDOM were highest, coinciding with the highest attenuation coefficients (Fig. 2). Average K_{PAR} ranged from a low of 0.54 m^{-1} at MM1 to a maximum of 2.76 m^{-1} at MM9 (Fig. 2). For 22% of surface light to reach 1.7 m depth corresponds to a K_{PAR} of 0.89 m^{-1} , indicated by the horizontal line in Fig. 2; K_{PAR} less than this indicates that 22% surface PAR can penetrate to a deeper depth. Stations downstream of MM4 generally had K_{PAR} values lower than 0.89 m^{-1} , except for samples collected during the fall season (Fig. 2). Stations landward of MM5 almost always had K_{PAR} values above this threshold, suggesting that seagrasses in the upper region of North River may be limited to shallower depths than 1.7 m because of light

limitation. Spatially averaged (mean±SD) K_{PAR} values were generally higher in summer ($1.29\pm0.849\text{ m}^{-1}$) and spring ($1.22\pm0.523\text{ m}^{-1}$), than in winter ($0.83\pm0.323\text{ m}^{-1}$) and fall ($1.07\pm0.370\text{ m}^{-1}$). Summer mean K_{PAR} values exhibited the steepest gradient from station MM1 to MM9 of all four seasons, while Fall mean K_{PAR} values were flat across sampling stations, with the exception of a high K_{PAR} at MM9 (Fig. 2). Growing season averages of K_{PAR} for each of the seagrass species were found to be lower for eelgrass, *Z. marina* ($K_{PAR} = 0.90 \pm 0.327\text{ m}^{-1}$, November–June) compared to *H. wrightii* ($K_{PAR} = 1.05 \pm 0.482\text{ m}^{-1}$, May–November) because of the higher water clarity observed during the winter season.

Turbidity showed the least trend across stations of the three optically significant water quality parameters. Spatial patterns in turbidity were strongest in summer, ranging from 5.09 NTU at MM1 to 20.77 NTU at MM9 (Fig. 2). Other seasons did not exhibit as strong a spatial trend; for instance, in fall, there was a slightly decreasing trend in

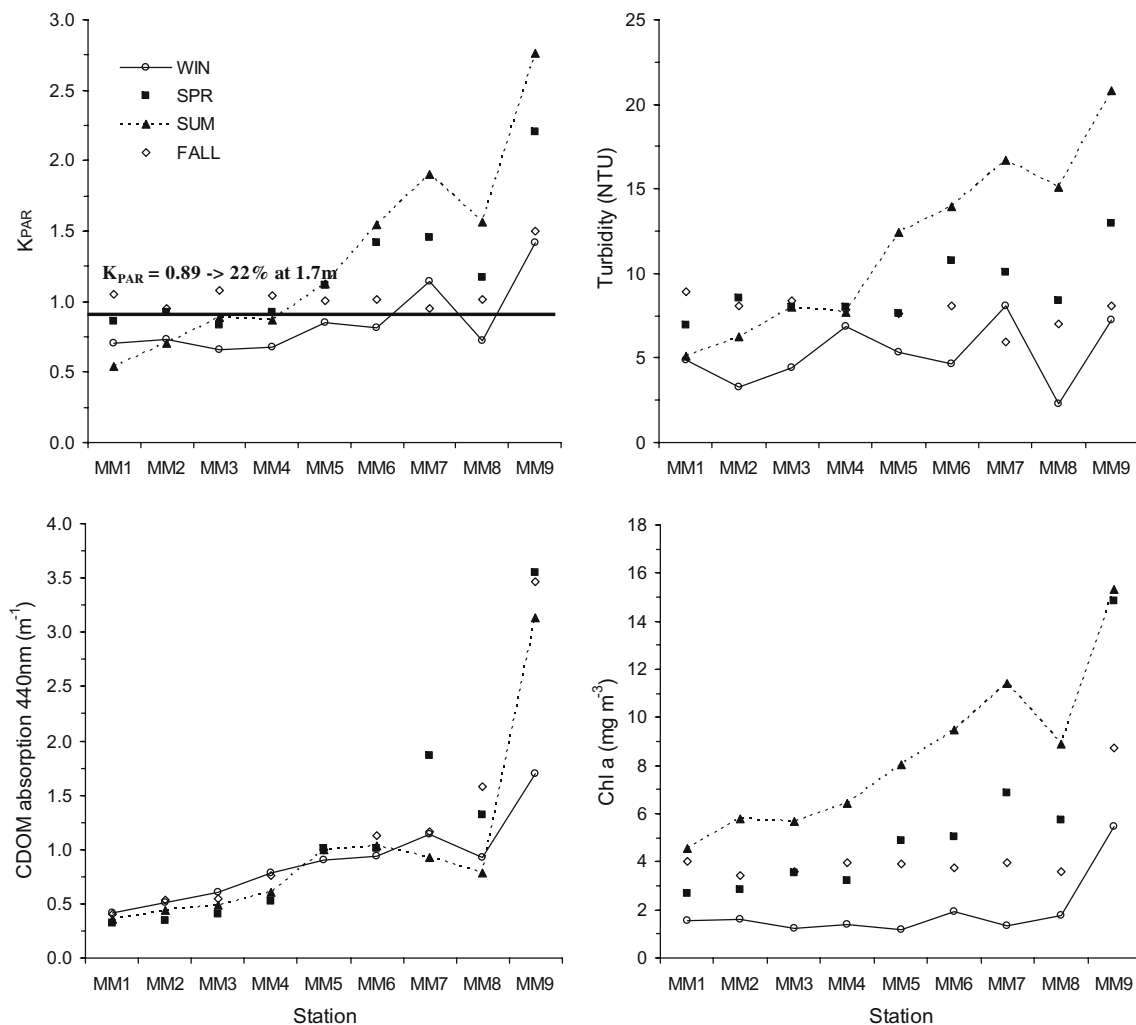


Fig. 2 Plots of seasonally averaged K_{PAR} and three apparent optical constituent values: turbidity, CDOM, and Chl *a* from North River, North Carolina. Data were collected at 4- to 6-week intervals from September 2002 to August 2004 at nine fixed stations along a water quality gradient

turbidity from MM1 (8.93 NTU) to MM9 (8.09 NTU). Turbidity was seasonally variable, with spatially average winter means (5.00 ± 4.068 NTU) lower than during the rest of the year: spring (9.09 ± 2.916 NTU), summer (11.98 ± 7.948 NTU), and fall (7.81 ± 4.691 NTU; Fig. 2). This corresponds with observations of lower attenuation coefficients at all stations during the months of December to February.

Chl *a* values were lowest in winter (2.18 ± 2.884 mg m⁻³) and highest in summer (8.29 ± 4.417 mg m⁻³) for all nine stations sampled, with fall (4.38 ± 4.346 mg m⁻³) and spring (5.59 ± 4.775 mg m⁻³) lying in between these two extremes (Fig. 2). In all four seasons, there tended to be an increase in Chl *a*, from a minimum (1.56 mg m⁻³ in winter) at MM1 to a maximum (15.35 mg m⁻³ in summer) at MM9 (Fig. 2), much like the pattern observed for both CDOM and turbidity.

CDOM absorption at 440 nm showed the most consistency of the three water quality parameters across seasons,

increasing at a similar rate from the downstream (MM1) to the upstream (MM9) stations (Fig. 2). The range of observed CDOM absorption was 0.319 m⁻¹ at MM1 to 3.554 m⁻¹ at MM9, both in the spring (Fig. 2). Spatially averaged CDOM values were comparable across seasons: winter (0.89 ± 0.482 m⁻¹), spring (1.16 ± 1.280 m⁻¹), summer (1.03 ± 1.508 m⁻¹), and fall (1.20 ± 1.111 m⁻¹), indicating that the spatial trend was dominant and suggesting that CDOM is less affected by seasonal changes than either turbidity or Chl *a*.

Calibration of the Bio-Optical Model

The scaling coefficients for Turb, $a_{\text{NTU}}^*(440)$, $b_{\text{NTU}}^*(555)$, and Chl *a*, $a_{\phi}^*(675)$, in the bio-optical model were determined by linear regression. The estimated $a_{\text{NTU}}^*(440)$ was 0.0384 m⁻¹ NTU⁻¹ ($r^2=0.61$; Fig. 3), and the scattering/turbidity ratio, $b_{\text{NTU}}^*(555)$, was 0.702 m⁻¹ NTU⁻¹ ($r^2=0.51$; Fig. 3). Higher degree of scatter was

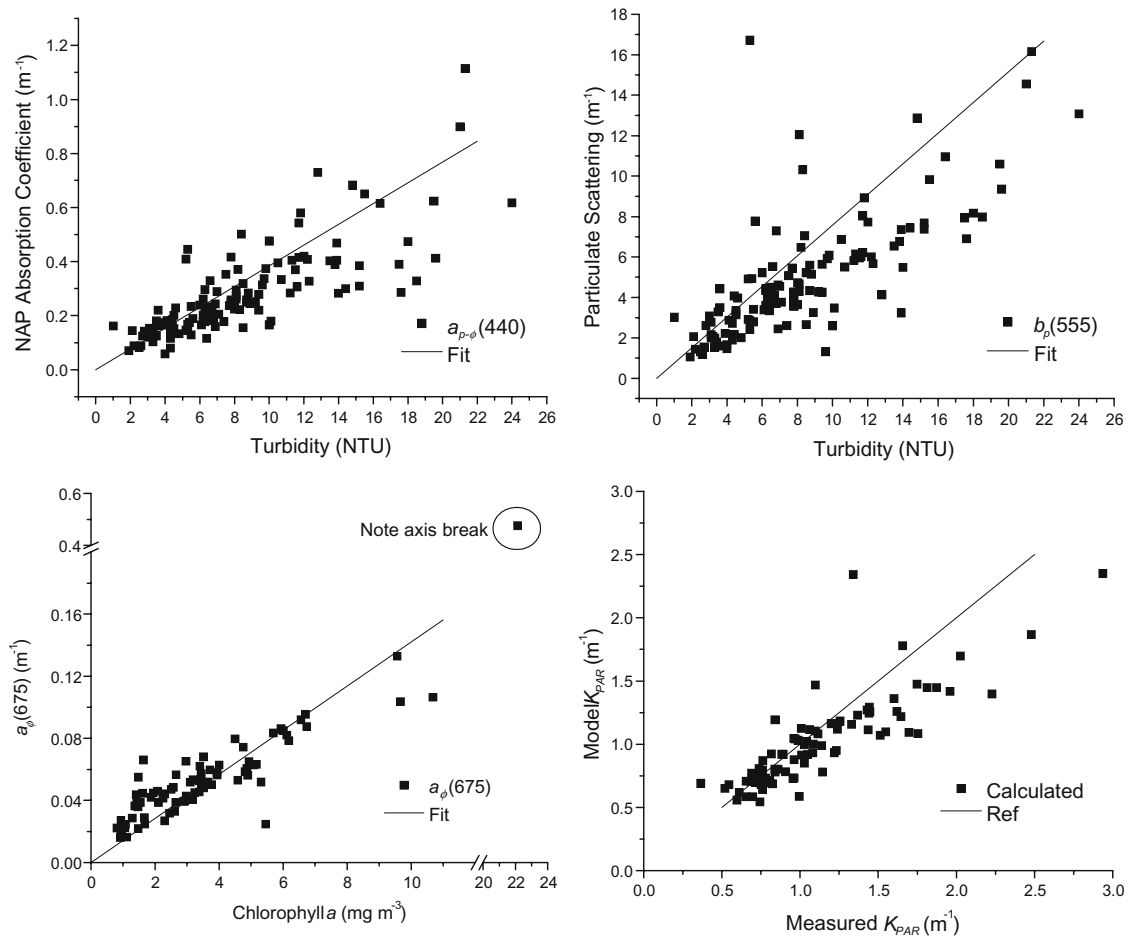


Fig. 3 Linear regressions between optical properties and water quality measurements: nonalgal particulate absorption at 440 nm, $a_{p-\phi}(440)$, vs turbidity; particulate scattering coefficient at 555 nm, $b_p(555)$, vs turbidity; and absorption by phytoplankton at 675 nm, $a_{\phi}(675)$, vs

chlorophyll *a*. Solid lines in $a_{p-\phi}(440)$, $b_p(555)$, and $a_{\phi}(675)$ are regression fits. Absorption and scattering relationships were then used to model light attenuation and compared with measured values of K_{PAR} , $r^2=0.707$. Solid line is line of 1:1 agreement for reference

present in the data as turbidity increased, partly because of fewer available observations, and may be indicative of a more variable particulate composition at the higher energy required to raise turbidity into the elevated NTU range. Absorption by Chl *a* was estimated at $a_{\phi}^*(675)=0.0136 \text{ m}^2 (\text{mg Chl } a)^{-1}$ ($r^2=0.59$; outlier suppressed because of excessive leverage; Fig. 3). The one outlier point where Chl *a* was measured at 22.12 mg m^{-3} was collected at MM9 in September 2002 during tropical storm Gustav, with sustained winds at 48 km h^{-1} , and may have been elevated because of suspension of benthic algae. The modeled K_{PAR} based on these IOPs underestimated the observed K_{PAR} by an average of 23% at high values (e.g., measured $K_{\text{PAR}} > 1.5 \text{ m}^{-1}$) but was largely unbiased (average percent error = -2%, average absolute percent error = 14%) in the range most relevant to determining seagrass depth limits, i.e., approximately 0.5 to 1.2 m^{-1} (Fig. 3). The negative bias at high K_{PAR} may be due, in part, to underestimation of the effect of NAPs in situ because of the vertical gradient in turbidity not being adequately represented in the sample from 0.5 m.

Components of Light Attenuation

The light attenuation coefficient, K_{PAR} , was partitioned into “partial attenuation coefficients” attributable to the three optically significant water quality parameters. The mean K_{PAR} over the 24-month study period ranged from 0.830 m^{-1} at station MM2 to 1.953 m^{-1} at MM9 (Fig. 4). The mean K_{PAR} increased upstream, caused by increases in the concentrations of all three water quality parameters (Figs. 2 and 4). The ranking of importance of the three parameters varied in the upstream direction, with turbidity contributing the most (45%) to K_{PAR} near Beaufort Inlet (MM1) and declining to 39% at MM9 (Fig. 4). CDOM contributed least (15%) to K_{PAR} at MM1 and increased in importance upstream, just surpassing turbidity at MM9 (42%; Fig. 4). The relative contribution to K_{PAR} by water declined from 21% at MM1 to 9% at MM9, while the contribution from chlorophyll varied only slightly, from 19 to 21%. This suggests that CDOM becomes increasingly important in driving overall light attenuation as one moves upstream toward its source in the salt marshes surrounding the upper regions of the North River.

Seagrass Water Column Light Requirement Thresholds

Inversion of the calibrated bio-optical model was used to produce WCLR threshold lines of constant attenuation for the APES (Fig. 5). Monthly water quality concentrations for the two manageable attenuating optical components (turbidity and Chl *a*) from the North River are plotted for stations MM4–MM6 against the predicted 22% WCLR

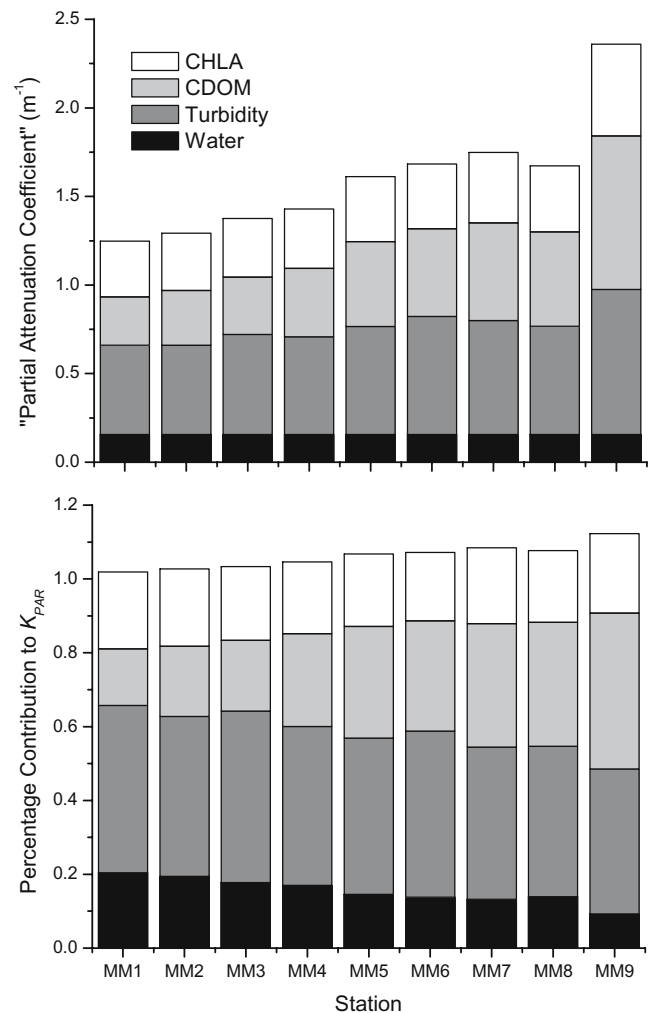


Fig. 4 Relative contributions of three water quality constituents (Chl *a*, CDOM, turbidity) to diffuse attenuation (K_{PAR}) for the nine stations. *Top panel* is partial attenuation coefficient over the 24-month study period; *bottom panel* is mean percentage contribution for each constituent

seagrass survival thresholds for 1-, 1.7-, and 2-m depths, respectively (Fig. 5). Most samples from stations MM4 to MM6, the midregion of North River where seagrasses are most abundant, fall in the region of acceptable light quantities ($\geq 22\%$ surface PAR) reaching 1.7 m depth (Fig. 5), except for one sample that was collected during storm conditions (September 2002) when turbidity values exceeded 20 NTU. This suggests that light attenuation in the middle portion of the North River is generally low enough to support seagrasses to a maximum depth of approximately 1.5 m as the annual mean and median K_{PAR} are 1.04 and 0.96 m^{-1} , respectively. K_{PAR} values protective of seagrass survival were less frequently seen in the upstream stations (MM7–MM9), where seagrass was observed to be sparse and occur only as fringing beds in the shallows near the eastern shoreline (Fig. 1).

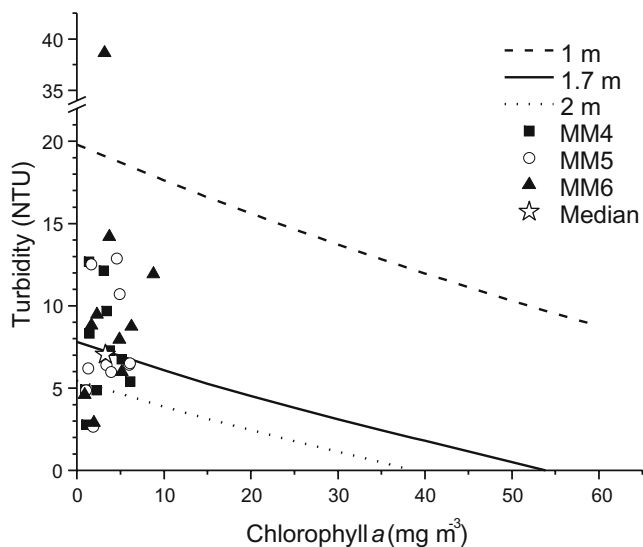
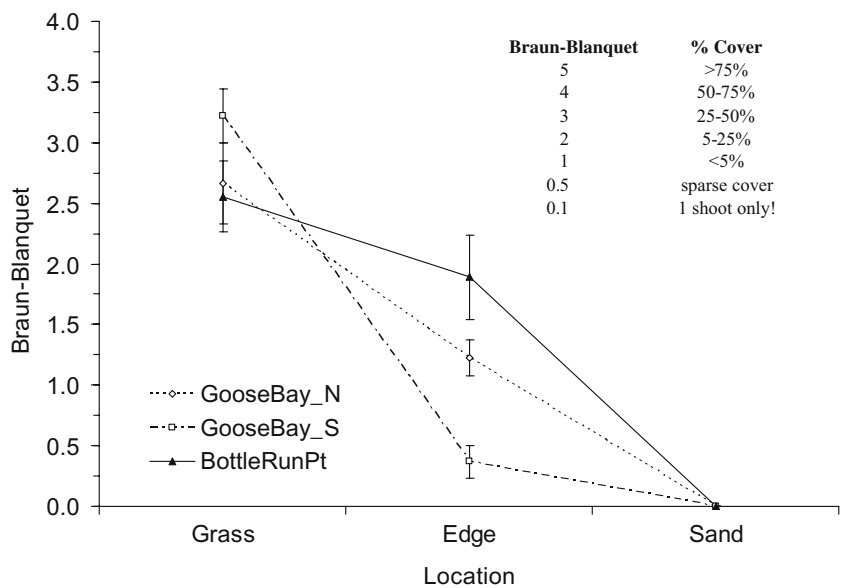


Fig. 5 Light-threshold model applied to selected North River water-quality data. Symbols represent monthly values collected at stations MM4–MM6 within North River; star, median value for all points. Threshold lines for three depths (1, 1.7, 2 m) predicted using the bio-optical model are plotted for comparison. Data points exceeding (above) a given threshold line indicate water quality that is not protective of seagrasses to that depth; that is, light is less than 22% of surface irradiance at that depth

Seagrass Surveys

At all three sites, GB-N, GB-S, and BRP, the seagrass coverage data showed a very distinct edge occurring over a 0.75-m distance, with on the average 25–50% cover of *H. wrightii* (shoalgrass) in the meadow, from very sparse to less than 25% cover on the deep edge, and 0% cover outside the meadow when using three adjacently located

Fig. 6 Braun–Blanquet density of seagrass along three deep edges in North River, North Carolina: Goose Bay North (GB-N), Goose Bay South (GB-S), and Bottle Run Point (BRP). The distance between the grass and the sand categories was 0.75 m



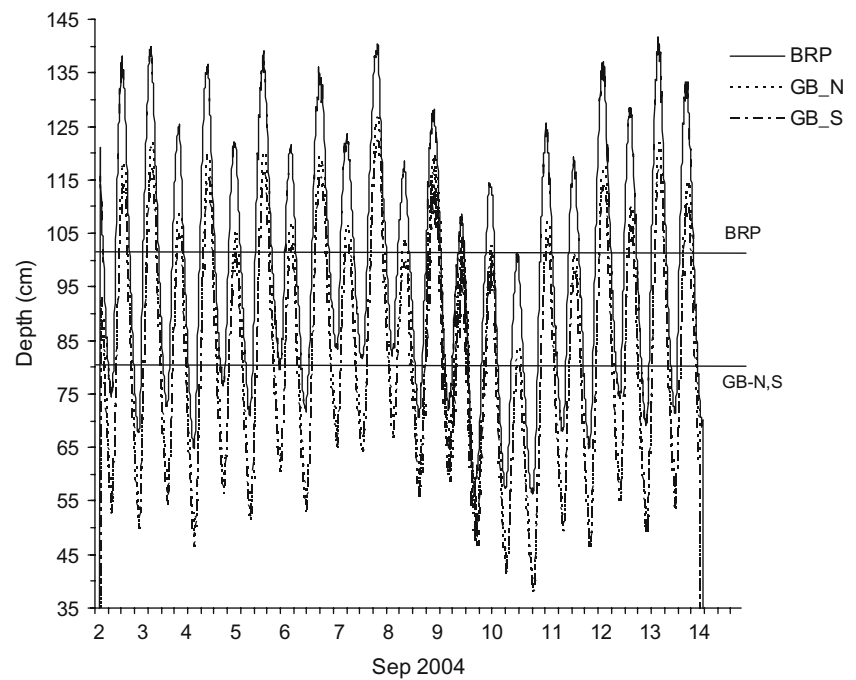
0.25 m² sampling quadrats over a transect distance of 0.75 m from grass to sand (Fig. 6). There was a less distinct edge at BRP, the most downstream site with lower K_{PAR} and deeper depths, compared to the very sharp edge in shallow depths found at GB-S (Fig. 6).

Water depths at the time of Braun–Blanquet assessments were ebbing based on the pressure sensor data. This was confirmed by the independent depth measurements at the three transects (Table 1) as well as by additional data (not reported in this paper) collected using the D-GPS carrier-phase technique of Johansson (2002). During the 12-day deployment, the mean tidal level was 0.80 m at GB-N, 0.79 m at GB-S, and 0.98 m at BRP (Table 1), with tidal amplitudes of 0.88, 0.84, and 0.86 m, respectively (NOAA 2001; station ID 8656483). The maximum water depth at high tide during the period of measurement was 1.27 m at GB-N, 1.22 m at GB-S, and 1.42 m at BRP (Fig. 7). The maximum depth of the deep edge of seagrass meadows found in North River occurred between 0.8 and 1.0 m, averaging 0.87 m local MSL; this was corroborated by the D-GPS measured absolute depth referenced to local MSL using the Trimble postprocessed data (Table 2). Adjusting this mean for the measured tidal amplitude of 0.86 m with the formula of Koch (2001) suggests that seagrasses in North River are restricted to a maximum water depth of about 1.35 m.

Discussion

A bio-optical model developed for predicting light attenuation and seagrass depth distribution from standard water quality measurements (Gallegos 1994) was successfully

Fig. 7 Tidal signal at the three study locations: Goose Bay North (GB-N), Goose Bay South (GB-S), and Bottle Run Point (BRP). Mean tide levels at the sites for the 2-week period before depth characterization in September 2004 are indicated by the two labeled horizontal lines



calibrated in North River, a subestuary of the larger APES system in North Carolina. The model was previously calibrated in the Chesapeake Bay (Gallegos 2001) and IRL, Florida (Gallegos and Kenworthy 1996). Calibration of the optical model in North River captured the range of likely water quality conditions found in the APES system, home to the second largest abundance of seagrass habitats in the continental USA (Street et al. 2005). As expected, recalibration of the absorption and attenuation coefficients in the model was necessary because of differences in the optical properties of the suspended sediments and phytoplankton and confirmed the need for regional calibration of the model. K_{PAR} is lower in the North River, North Carolina, than in the Rhode River, Maryland (Gallegos et al. 1990; Gallegos 1994), because of lower chlorophyll concentrations and lower ratio of NAP absorption/turbidity [i.e., lower $a_{NTU}^*(440)$] in the North River. It is interesting to note that the ranges of turbidity were quite similar between the North River and Rhode River (cf. Fig. 2a in Gallegos 1994), but the lower value for $a_{NTU}^*(440)$ in the North River resulted in lower K_{PAR} values there because diffuse attenuation responds to the square root of the scattering coefficient, despite a roughly linear response to the absorption coefficient (Kirk 1994).

We hypothesize that the main difference in optical properties between the North River and Rhode River is due to changes in particle size and composition. Our value of $a_{NTU}^*(440)$ was lower than that of Gallegos (1994) by a factor of greater than 6. In the lower North River, near the inlet, sediments are characterized by quartz sands, while in

the upper portion of the estuary, sediments were observed to be dominated by fine silts and mud (Kenworthy et al. 1982; Fonseca and Bell 1998). Silt and mud sediments dominate in the low-energy Rhode River (Gallegos et al. 2005). Differences in particle composition and size drive changes in the absorption and scattering properties of the medium. Babin et al. (2003) found approximately 20-fold variability in individual measurements of specific scattering coefficients from various coastal and oceanic regions, with regional means varying twofold between coastal and oceanic regions. The results of these optical comparisons between Chesapeake Bay and APES and the investigation into the effects of particle composition on optical properties suggest that regional calibrations of bio-optical models are important if this tool is to be correctly applied in making predictions about seagrass habitat suitability.

Absorption and scattering properties of NAPs measured in the laboratory were better correlated with in situ turbidity measurements using a YSI 6136 optical probe than with TSS measured in the surface water samples. We therefore calibrated absorption and scattering by NAPs in the bio-optical model in terms of turbidity. We surmise two main reasons for this discrepancy; firstly, in samples from marine waters, it is necessary to flush all salts from the filter to generate an accurate weight of sediments in the sample. However, this may be difficult as the approach calls for filtering a water sample until the filter is nearly “clogged” to maximize the weight of sediments; running additional rinse water through this filter can become challenging. Secondly, and more importantly, is the sediment particle

size and composition. For a given mass concentration of suspended sediments, the scattering and absorption coefficients increase as the particle size distribution is shifted to finer particle sizes (Stramski et al. 2002; Babin and Stramski 2004). We would expect therefore that energy regimes favoring suspension of fine silts and clays would have higher mass-specific absorption and scattering coefficients than more energetic conditions favoring suspension of heavy sand-sized particles. Strong variability in tides and wind-driven currents can be expected to produce wide variability in mass-specific absorption and scattering coefficients based on concentrations of TSS. In contrast, the turbidity reading is ultimately derived from a measure of light backscattering by particles in suspension. Therefore, to a degree, the turbidity associated with a given mass concentration of suspended solids will vary with changes in particle size distribution in the same direction as the absorption and scattering per unit mass. Because of these methodological issues with TSS, we found that turbidity was a better indicator to scale the IOPs of NAPs than TSS. This is also a benefit to comparing the optical model thresholds with data from monitoring programs, which routinely use the Environmental Protection Agency (EPA)-approved method for turbidity measurements (O'Dell 1993). However, the disadvantage of basing an optical model on turbidity is that, unlike TSS, turbidity is not amenable to mass transport modeling.

Our calibration of the optical model as a tool for assessing habitat suitability for seagrasses in the wider APES system was derived from monitoring data collected in the much smaller North River. The North River system was chosen because it spanned the range of optical properties that are likely to be encountered by seagrasses in the APES. That is, both high clarity water from oceanic exchange through Beaufort Inlet and highly colored and turbid waters up in the marsh-fringed shallow portion of North River were sampled to span the range of potential water quality conditions. However, it was experimentally more tractable to sample than the entire APES system because of the smaller size and ease of access. Furthermore, sampling occurred on both flood and ebb tides and in a range of weather conditions, including storms and very calm days. In 2 months (September 2002 and March 2003), samples were collected during storm conditions, tropical storm Gustav with 48 km h^{-1} , and a northeaster with 40-km h^{-1} -sustained wind speeds reported from the Cape Lookout (CLKN7) weather station. These events produced some of the highest turbidity and correspondingly high K_{PAR} values observed in the data, indicating the importance of natural events in driving extreme values in this shallow estuarine system. Other shallow estuaries should be similar (see, e.g., Moore et al. 1997).

Because the seagrass WCLR target of the model is driven in large part by light availability, K_{PAR} is a convenient measure of habitat quality. It is primarily the light-limited deep edge of seagrass meadows that will respond to variations in K_{PAR} and therefore influence the distribution and density of the meadows (Dennison and Alberte 1982, 1985; Kenworthy and Fonseca 1996). We found that maximum depth of the deep edge of seagrass meadows in North River occurred between 0.8 and 1.0 m, averaging 0.87 m local MSL. Adjusting for tidal amplitude using the formula of Koch (2001) suggests that seagrasses in North River are restricted to a maximum water depth of about 1.35 m on average. Observations made on the multidecadal distribution of seagrass beds in this estuary since the early 1970s suggest that the deep-edge depth has not changed substantially (Kenworthy et al. 1982). In the North River where the bio-optical model was calibrated, it predicted a deeper depth distribution (1.7 m MSL) for seagrasses than was observed (0.87 m MSL). North River seagrass meadows are generally shallower than the deep edges reported from the larger and more extensively vegetated Core Sound (Ferguson and Korfmacher 1997; Field, personal communication). Core Sound is more representative of the widely distributed seagrass beds in the high salinity region of APES (Street et al. 2005) than North River.

The deepest edges in Core Sound are approximately 1.2 m on the more turbid mainland shoreline (western) and 2.0 m on the barrier island side (eastern shoreline) where light attenuation is typically lower (Table 2). Based on mean water quality conditions, the optical model predicted 22% light reaching a depth of 1.7 m for the APES (Fig. 5), which is about the range of maximum depths (1.7–2.0 m) reported from the eastern Core Sound seagrass meadows, where 71% of seagrass meadows were deeper than 1.0 m (Ferguson and Korfmacher 1997). Maximum seagrass depth limits in North River were more comparable with the mainland side of Core Sound (0.87 vs 1.2 m). Along the mainland coast, Ferguson and Korfmacher (1997) reported seagrass meadows as narrow linear features in very shallow water, much like that we observed in North River. Only 23% of seagrass meadows mapped occurred at depths greater than 1.0 m, and all were less than 1.2 m in the mainland section. These results illustrate the importance of location along the water quality gradient from inshore to offshore conditions in the APES in determining maximum seagrass depth limits.

Many of the seagrass meadows in North River are associated with sheltered lagoons occurring in the Middle and North River Marshes and so may not have a light-limited “deep edge” because they are in shallow basins. Other meadows are found adjacent to deep tidal channels

with highly dynamic sandy sediments possibly representing energy-limited edges, rather than light-limited ones. Seagrasses within Core Sound are less affected by tidal energy, being more exposed to wind and wave action (Fonseca and Bell 1998), than are the meadows in North River. The calibrated model appears to be a robust predictor of depth limits for seagrasses in the eastern APES system, despite local variability in factors other than light that affect the depth to which the plants can be found.

We envision the optical model being used as a tool that assists managers to set water quality goals to protect diminishing seagrass habitats in the APES. Criteria from our model can now be used by the State of North Carolina to set guidelines for optically significant water quality parameters that are protective of seagrasses. A recent revision of the state's Coastal Habitat Protection Plan introduced the idea of using the bio-optical model to set these criteria (Street et al. 2005). With this calibrated model and demonstrated applicability in three regions along the US eastern coastline, this tool is ready to be adopted in assisting managers and researchers with developing criteria and evaluating water quality-monitoring results.

Although past model calibrations utilized TSS as one of the primary input water quality variables (Gallegos 2001; Gallegos and Neale 2002), we successfully calibrated the model with turbidity as an indicator of particulates. Turbidity has an EPA standard method that is easier to measure than TSS, is less expensive, more widely used by water quality agencies, and can be continuously monitored with available probes. With routine measurements of turbidity, Chl *a*, and CDOM, one can now predict the light attenuation coefficient under different combinations of these water quality parameters. Chl *a* is already routinely measured by almost all monitoring programs and has a well-accepted EPA standard method. Unfortunately, CDOM absorption is less routinely measured, yet it is an important OAC. Measurement of absorption on a 0.22- μm -filtered water sample is preferable to the visual comparison with platinum color standards (Cuthbert and del Giorgio 1992). In instances where color is an important component of attenuation, e.g., APES and St John's River, FL (Gallegos 2005), it is especially important to sample this variable. Measurement of CDOM absorption by published protocols (Mitchell et al. 2002) should be adopted as a routine parameter by managers tasked with water quality monitoring for optically important water quality parameters and to help determine criteria that are protective of seagrasses.

Calibration of the optical model requires expertise in radiative transfer modeling in the underwater environment (Mobley 1994) and access to an instrument such as the Wetlabs ac-9 to generate scaling factors for absorption and scattering coefficients in relation to water quality measure-

ments. We suspect that this level of expertise is currently outside the regular purview of many management agencies and recommend that this be undertaken in conjunction with scientists or engineers well versed in the field. Nonetheless, this collaborative approach has been successful in a number of regions where concern over water quality and seagrass losses has resulted in adoption of water quality criteria based on OAC to help evaluate monitoring results and set targets for management. These include collaborations in the Chesapeake Bay (Kemp et al. 2004), the subtropical IRL (Steward et al. 2005), and the successful recovery of seagrasses in Tampa Bay after dramatic nutrient reductions (Johansson and Lewis 1992; Miller and McPherson 1995; Robbins 1997).

Once model calibration is done, however, use of standard monitoring techniques (e.g., PAR meters and YSI optical probes) may be sufficient to determine whether water quality meets seagrass habitat requirements. This bio-optical tool is important to management and research agencies tasked with protection of aquatic habitats and should be expanded to address other regions of the USA with similar natural resources. An atlas of calibrated optical models specific to regions and/or local conditions should be produced and widely disseminated. The first step toward such a product will be the publication of the results of a comparative evaluation of model calibrations for the Chesapeake Bay, APES, and IRL regions.

Acknowledgments Grateful thanks to the cadre of persons who were instrumental in assisting with data collection in the field, including staff and interns at the Center for Coastal Fisheries and Habitat Research, students and technicians at the Institute of Marine Science, staff at Smithsonian Environmental Research Center, and numerous volunteers. Boat support was provided by the Center for Coastal Fisheries and Habitat Research, NCCOS, NOS, NOAA, Beaufort, NC. This research was funded by EPA-STAR grants (R82867701) to the ACE-INC EaGLes Center (www.aceinc.org) and (R82868401) to the Atlantic Slope Consortium EaGLes Center (www.asc.psu.edu).

References

- Abal, E., and W. Dennison. 1996. Seagrass depth range and water-quality in southern Moreton Bay, Queensland, Australia. *Marine and Freshwater Research* 47: 763–771.
- Agusti, E.S., S. Enriquez, H. Frost-Christensen, K. Sand-Jensen, and C.M. Duarte. 1994. Light-harvesting among photosynthetic organisms. *Functional Ecology* 8: 273–279.
- Babin, M., and D. Stramski. 2002. Light absorption by aquatic particles in the near-infrared spectral region. *Limnology and Oceanography* 47: 911–915.
- Babin, M., and D. Stramski. 2004. Variations in the mass-specific absorption coefficient of mineral particles suspended in water. *Limnology and Oceanography* 49: 756–767.
- Babin, M., A. Morel, V. Fournier-Sicre, F. Fell, and D. Stramski. 2003. Light scattering properties of marine particles in coastal

- and open ocean waters as related to the particle mass concentration. *Limnology and Oceanography* 48: 843–859.
- Batiuk, R.A., P. Bergstrom, M. Kemp, E. Koch, L. Murray, J.C. Stevenson, R. Bartleson, V. Carter, N.B. Rybicki, J.M. Landwehr, C. Gallegos, L. Karrh, M. Naylor, D. Wilcox, K.A. Moore, S. Ailstock, and M. Teichberg. 2000. *Chesapeake Bay submerged aquatic vegetation water quality and habitat-based requirements and restoration targets: a second technical synthesis. Chesapeake Bay Program, CBP/TRS 245/00*. Annapolis, MD: US Environmental Protection Agency.
- Biber, P.D., H.W. Paerl, C.L. Gallegos, and W.J. Kenworthy. 2005. Evaluating indicators of seagrass stress to light. In *Estuarine indicators*, ed. , 193–210. Boca Raton, FL: CRC.
- Buzzelli, C.P., J. Ramus, and H.W. Paerl. 2003. Ferry-based monitoring of surface water quality in North Carolina estuaries. *Estuaries* 26: 975–984.
- Carraway, R.J., and L.J. Priddy. 1983. *Mapping of submerged grass beds in Core and Bogue Sounds, Carteret County, North Carolina, by conventional aerial photography. CEIP Report no. 20*. Raleigh, NC: North Carolina Department of Natural Resources and Community Development.
- Carter, V., N. Rybicki, J. Landwehr, and M. Naylor. 2000. Light requirements for SAV survival and growth. In *Chesapeake Bay submerged aquatic vegetation water quality and habitat-based requirements and restoration targets: a second technical synthesis, Chesapeake Bay Program, CBP/TRS 245/00*, eds. R.A. Batiuk, P. Bergstrom, M. Kemp, et al., 11–34. Annapolis, MD: US Environmental Protection Agency.
- Cuthbert, I.D., and P. del Giorgio. 1992. Toward a standard method of measuring color in freshwater. *Limnology and Oceanography* 37: 1319–1326.
- Dennison, W., and R. Alberte. 1982. Photosynthetic responses of *Zostera marina* L. (eelgrass) to in situ manipulations of light intensity. *Oecologia* 55: 137–144.
- Dennison, W., and R. Alberte. 1985. Role of daily light period in the depth distribution of *Zostera marina* (eelgrass). *Marine Ecology Progress Series* 25: 51–61.
- Dennison, W., R. Orth, K. Moore, J. Stevenson, V. Carter, S. Kollar, P. Bergstrom, and R.A. Batiuk. 1993. Assessing water quality with submersed aquatic vegetation. *Bioscience* 43: 86–95.
- Dixon, L.K. 2000. Establishing light requirements for the seagrass *Thalassia testudinum*: an example from Tampa Bay, Florida. In *Seagrasses: monitoring, ecology, physiology and management*, ed. , 9–32. Boca Raton, FL: CRC.
- Duarte, C. 1991. Seagrass depth limits. *Aquatic Botany* 40: 363–377.
- Ferguson, R., and K. Korfmacher. 1997. Remote sensing and GIS analysis of seagrass meadows in North Carolina, USA. *Aquatic Botany* 58: 241–258.
- Ferguson, R.L., and L.L. Wood. 1994. *Rooted vascular aquatic beds in the Albemarle-Pamlico estuarine system. Cooperative Agreement between U.S. Environmental Protection Agency through the State of North Carolina, Albemarle-Pamlico estuary Study, and the National Marine Fisheries Service. Project/Report no. 94-02*. Beaufort, NC: National Oceanographic and Atmospheric Administration.
- Fonseca, M., and S. Bell. 1998. Influence of physical setting on seagrass landscapes near Beaufort, North Carolina, USA. *Marine Ecology Progress Series* 171: 109–121.
- Gallegos, C.L. 1994. Refining habitat requirements of submersed aquatic vegetation: Role of optic models. *Estuaries* 17: 187–199.
- Gallegos, C.L. 2001. Calculating optical water quality targets to restore and protect submersed aquatic vegetation: Overcoming problems in partitioning the diffuse attenuation coefficient for photosynthetically active radiation. *Estuaries* 24: 381–397.
- Gallegos, C.L. 2005. Optical water quality of a blackwater river estuary: the Lower St. Johns River, Florida, USA. *Estuarine, Coastal and Shelf Science* 63: 57–72.
- Gallegos, C.L., and P.D. Biber. 2004. Diagnostic tool sets water quality targets for restoring submerged aquatic vegetation in Chesapeake Bay. *Ecological Restoration* 22: 296–297.
- Gallegos, C.L., D.L. Correll, and J.W. Pierce. 1990. Modeling spectral diffuse attenuation, absorption, and scattering coefficients in a turbid estuary. *Limnology and Oceanography* 35: 1486–1502.
- Gallegos, C.L., T.E. Jordan, A.H. Hines, and D.E. Weller. 2005. Temporal variability of optical properties in a shallow, eutrophic estuary: Seasonal and interannual variability. *Estuarine, Coastal and Shelf Science* 64: 156–170.
- Gallegos, C.L., and W.J. Kenworthy. 1996. Seagrass depth limits in the Indian River Lagoon (Florida, U.S.A.): Application of an Optical Water Quality Model. *Estuarine, Coastal and Shelf Science* 42: 267–288.
- Gallegos, C.L., and K. Moore. 2000. Factors contributing to water-column light attenuation. In *Chesapeake Bay submerged aquatic vegetation water quality and habitat-based requirements and restoration targets: a second technical synthesis, Chesapeake Bay Program, CBP/TRS 245/00*, eds. , and P. Bergstrom Annapolis, MD: US Environmental Protection Agency.
- Gallegos, C.L., and P. Neale. 2002. Partitioning spectral absorption in case 2 waters: discrimination of dissolved and particulate components. *Applied Optics* 41: 4220–4233.
- Gattuso, J.P., B. Gentili, C.M. Duarte, J.A. Kleypas, J.J. Middelburg, and D. Antoine. 2006. Light availability in the coastal ocean: impact on the distribution of benthic photosynthetic organisms and their contribution to primary production. *Biogeosciences* 3: 498–513.
- Green, F.P., and F.T. Short. 2003. *World atlas of seagrasses*. Berkeley, CA: University of California Press.
- Hemminga, M.A., and C. Duarte. 2000. *Seagrass ecology*. Cambridge, UK: Cambridge University Press.
- Hench, J.L., and R.A. Luettich. 2003. Transient tidal circulation and momentum balances at a shallow inlet. *Journal of Physical Oceanography* 33: 913–932.
- Johansson, J. 2002. Water depth (MTL) at the deep edge of seagrass meadows in Tampa Bay measured by GPS carrier-phase processing: evaluation of the technique. In *Seagrass management: it's not just nutrients!*, ed. , 151–168. St. Petersburg, FL: Tampa Bay Estuary Program.
- Johansson, J.O.R., and R.R. Lewis. 1992. Recent improvements of water quality and biological indicators in Hillsborough Bay, a highly impacted subdivision of Tampa Bay, Florida, USA. *Science of the Total Environment Supplement* 1992: 1199–1215.
- Kemp, W.M., R. Batiuk, R. Bartleson, P. Bergstrom, V. Carter, C.L. Gallegos, and W. Hunley. 2004. Habitat requirements for submerged aquatic vegetation in Chesapeake Bay: Water quality, light regime, and physical-chemical factors. *Estuaries* 27: 363–377.
- Kenworthy, W.J., and D.E. Haurert. 1991. *The light requirements of seagrasses: proceedings of a workshop to examine the capability of water quality criteria, standards and monitoring programs to protect seagrasses. National Oceanographic and Atmospheric Administration (NOAA) Technical Memorandum NMFS-SEFC-287*. Silver Spring, MD: National Oceanographic and Atmospheric Administration.
- Kenworthy, W.J., and M.S. Fonseca. 1996. Light requirements of seagrasses *Halodule wrightii* and *Syringodium filiforme* derived from the relationship between diffuse light attenuation and maximum depth distribution. *Estuaries* 19: 740–750.
- Kenworthy, W.J., J.C. Zieman, and G.W. Thayer. 1982. Evidence for the influence of seagrasses on the benthic nitrogen cycle in a

- coastal plain estuary near Beaufort, North Carolina (USA). *Oecologia* 54: 152–158.
- Kirk, J.T.O. 1980. Relationship between nephelometric turbidity and scattering coefficients in certain Australian Waters. *Australian Journal of Marine and Freshwater Research* 31: 1–12.
- Kirk, J.T.O. 1988. Optical water quality—what does it mean and how should we measure it? *Journal of the Water Pollution Control Federation* 60: 194–197.
- Kirk, J.T.O. 1994. *Light & photosynthesis in aquatic ecosystems*. Cambridge, UK: Cambridge University Press.
- Kishino, M., M. Takahashi, N. Okami, and S. Ichimura. 1985. Estimation of the spectral absorption coefficients of phytoplankton in the sea. *Bulletin of Marine Science* 37: 634–642.
- Koch, E.W. 2001. Beyond light: physical, geological and geochemical parameters as possible submersed aquatic vegetation habitat requirements. *Estuaries* 24: 1–17.
- Larkum, A.W.D., R.J. Orth, and C.M. Duarte. 2006. *Seagrasses: biology, ecology and conservation*. Amsterdam: Springer.
- Lin, J., L. Xie, L.J. Pietrafesa, J.S. Ramus, and H.W. Paerl. 2007. Water quality gradients across Albemarle-Pamlico estuarine system: seasonal variations and model applications. *Journal of Coastal Research* 23: 213–229.
- Markager, S., and K. Sand-Jensen. 1992. Light requirements and depth zonation of marine macroalgae. *Marine Ecology Progress Series* 88: 83–92.
- Markager, S., and K. Sand-Jensen. 1994. The physiology and ecology of light–growth relationship in macroalgae. *Progress in Phycological Research* 10: 209–298.
- Markager, S., and K. Sand-Jensen. 1996. Implications of thallus thickness for growth irradiance relationships of marine macroalgae. *European Journal of Phycology* 31: 79–87.
- Miller, R.L., and B.F. McPherson. 1995. Modeling photosynthetically active radiation in water of Tampa Bay, Florida, with emphasis on the geometry of incident irradiance. *Estuarine, Coastal and Shelf Science* 40: 359–377.
- Mitchell, B.G., M. Kahru, J. Wieland, and M. Stramska. 2002. Determination of spectral absorption coefficients of particles, dissolved material and phytoplankton for discrete water samples. In *Ocean optics protocols for satellite ocean color sensor validation, rev. 4, vol 4: inherent optical properties: instruments, characterization, field measurements and data analysis protocols*. National Aeronautic and Space Administration (NASA) TM-2003. Goddard Space Flight Space Center, eds. , G.S. Fargion, and C.R. McClain, 39–64. Greenbelt, MD: National Aeronautic and Space Administration, Goddard Space Flight Space Center.
- Mobley, C.D. 1994. *Light and water: radiative transfer in natural waters*. New York: Academic.
- Moore, K.A., R.L. Wetzel, and R.J. Orth. 1997. Seasonal pulses of turbidity and their relations to eelgrass (*Zostera marina*) survival in an estuary. *Journal of Experimental Marine Biology and Ecology* 215: 115–134.
- Morel, A., and S. Maritorena. 2001. Bio-optical properties of oceanic waters: A reappraisal. *Journal of Geophysical Research* 106C: 7163–7180.
- Morris, L.J., R.W. Virnstein, J.D. Miller, and L.M. Hall. 2000. Monitoring seagrass changes in Indian River lagoon, Florida using fixed transects. In *Seagrasses: monitoring, ecology, physiology, and management*, ed. , 167–176. Boca Raton, FL: CRC.
- National Aeronautic and Space Administration (NASA), 2002. ER-2FSR Archive: NASA High Altitude Mission Branch, Flight Summary Reports, 2002 Flight Summary Reports. <http://asapdata.arc.nasa.gov/Fsr02.htm>. Accessed 26 Nov 2007.
- National Oceanic and Atmospheric Administration (NOAA), 2001. NOAA Tides and Currents. Center for Operational Oceanographic Products and Services. <http://tidesandcurrents.noaa.gov/nwlon.html>. Accessed 26 Nov 2007.
- National Oceanic and Atmospheric Administration (NOAA), 2003. 2003 precipitation data: National Weather Service Forecast Office, Newport/Morehead City, North Carolina. <http://www.erh.noaa.gov/mhx/2003Precip.html>. Accessed 26 Nov 2007.
- O'Dell, J.W. 1993. *Method 180.1: determination of turbidity by nephelometry. Revision 2.0. Environmental Monitoring Systems Laboratory*. Cincinnati, OH: Office of Research and Development, US Environmental Protection Agency.
- Onuf, C.P. 1996. Seagrass responses to long-term light reduction by brown tide in upper Laguna Madre, Texas: distribution and biomass patterns. *Marine Ecology Progress Series* 138: 219–231.
- Pilkey, O., and M. Fraser. 2003. *A celebration of the world's barrier islands*. New York: Columbia University Press.
- Robbins, B.D. 1997. Quantifying temporal change in seagrass aerial coverage: the use of GIS and low resolution aerial photography. *Aquatic Botany* 58: 259–267.
- Steward, J.S., R.W. Virnstein, L.J. Morris, and E.F. Lowea. 2005. Setting seagrass depth, coverage, and light targets for the Indian River Lagoon System, Florida. *Estuaries* 28: 923–935.
- Stramski, D., M. Babin, and S.B. Wozniak. 2002. Variations in the absorption coefficient of mineral particles caused by changes in the particle size distribution and refractive index. In *Proceedings of the XVI Ocean Optics Conference*, eds. S. Ackelson and C. Tree, Santa Fe, NM, 26–27.
- Street, M.W., A.S. Deaton, W.S. Chappell, and P.D. Mooreside. 2005. Submerged aquatic vegetation. In *North Carolina Coastal Habitat Protection Plan, North Carolina Department of Environment and Natural Resources*, eds. , A.S. Deaton, W.S. Chappell, and P.D. Mooreside, 253–310. Morehead City, NC: Division of Marine Fisheries.
- Susman, K.R., and S.D. Heron. 1979. Evolution of a barrier island, Shackleford Banks, Carter County, North Carolina. *Geological Society of America Bulletin* 90: 205–215.
- Thayer, G.W., W.J. Kenworthy, and M.S. Fonseca. 1984. *The ecology of eelgrass meadows of the Atlantic Coast: a community profile*. FWS/OBS-84/02. Washington, DC: US Fish and Wildlife Service.
- Tzortziou, M., J.R. Herman, C.L. Gallegos, P.J. Neale, A. Subramaniam, L.W. Harding, and Z. Ahmad. 2006. Bio-optics of the Chesapeake Bay from measurements and radiative transfer closure. *Estuarine, Coastal and Shelf Science* 68: 348–362.
- Virnstein, R.W., and L.J. Morris. 2000. Setting seagrass targets for the Indian River lagoon, Florida. In *Seagrasses: monitoring, ecology, physiology, and management*, ed. , 211–218. Boca Raton, FL: CRC.